Time Domain Analysis of Homogenized Finite Element Method for Eddy Current Analysis with Reduced Unknown Variables

Shingo Hiruma[1,2], Hajime Igarashi[1], *IEEE Member*

[1]Graduate School of Information Science and Technology, Hokkaido University, Hokkaido 060-0814, Japan
[2]Research Fellow of Japan Society for the Promotion of Science (JSPS), Tokyo 102-0083, Japan

This paper presents a new method for time-domain analysis based on the homogenized finite element method (FEM). The permeability in the homogenized domain is expressed by the Cauer equivalent circuit. The auxiliary unknowns relevant to the Cauer circuit are then eliminated using the finite difference method. The homogenized FE equation without the auxiliary unknowns can be effectively solved.

***Index Terms*—Cauer equivalent circuit, Complex permeability, Homogenization method, Multi-scale problem, Time-domain analysis.**

I. Introduction

In electric apparatus, fine structure material such as a silicon-steel sheet, litz wire, and soft magnetic composite are widely used to reduce eddy current losses. Recently, it has become more important to evaluate the eddy current losses because of increase in the switching speed of electric power devices. It needs, however, large computational cost to evaluate them in the fine structure materials using the conventional finite element method (FEM) because substantial number of finite elements, which have to be smaller than the skin depth, are involved. This problem, referred to as the multi-scale problem, is attributed to the scale difference between the overall size of electric apparatus and size of components such as the wire and magnetic powder.

To tackle this problem, homogenization method [1]–[5] has been proposed. In the method, fine structure material is modeled as uniform material which has the complex permeability. Thanks to the homogenization method, the fine-structured materials can be modeled by FEM without considering skin depth, and thus they can be analyzed with lower computational costs. The homogenization method has, however, a weak point that it is not straightforward to perform the time domain analysis because the complex permeability is a complex function formulated in frequency domain. The time domain analysis is indispensable when quasi-static electromagnetic field is analyzed considering the magnetic saturation. Although the time-domain homogenized FEM has been already proposed [6], [7], it depends on the low frequency approximation of the complex permeability. Therefore, its accuracy would be deteriorated as the driving frequency becomes higher.

Manuscript received April 1, 2015; revised May 15, 2015 and June 1, 2015; accepted July 1, 2015. Date of publication July 10, 2015; date of current version July 31, 2015. (Dates will be inserted by IEEE; "published" is the date the accepted preprint is posted on IEEE Xplore®; "current version" is the date the typeset version is posted on Xplore®). Corresponding author: F. A. Author (e-mail: f.author@nist.gov). If some authors contributed equally, write here, "F. A. Author and S. B. Author contributed equally." IEEE TRANSACTIONS ON MAGNETICS discourages courtesy authorship; please use the Acknowledgment section to thank your colleagues for routine contributions.

Color versions of one or more of the figures in this paper are available online at http://ieeexplore.ieee.org.

Digital Object Identifier (inserted by IEEE).

To overcome this difficulty, the complex permeability is represented by the Cauer circuit which is accurate over wide frequency range [8], [9]. In [8], the circuit equations for several auxiliary unknowns are coupled with the FE equation. Because the circuit equation is considered in all the finite elements in the homogenized region, a number of auxiliary unknowns are involved. To solve this problem, we propose here a new method for the homogenized FEM in time domain which avoids solution of the circuit equation in the transient computation. We apply the proposed method to the analysis of an inductor with a multi-turn coil. The numerical results are compared with the result obtained by the conventional FEM.

II. Formulation

A. Frequency domain homogenized FEM

Let us consider the homogenized FE equation which includes the complex permeability $\langle\dot{\mu}\rangle(s)$ that is a function of complex frequency s

$$K(\langle\dot{\nu}\rangle)\dot{\boldsymbol{x}}(s) = \boldsymbol{b}i, \tag{1a}$$

$$(K\dot{\boldsymbol{x}})_i = \sum_j K_{ij}\dot{a}_j = \sum_j \int_\Omega \mathrm{rot}\boldsymbol{N}_i \cdot \nu \mathrm{rot}\boldsymbol{N}_j d\Omega\, \dot{a}_j, \tag{1b}$$

$$b_i = \int_\Omega \boldsymbol{N}_i \cdot \boldsymbol{j} d\Omega \tag{1c}$$

where $\dot{\boldsymbol{x}}(s) = [\dot{a}_1, \dot{a}_2, \cdots]^{\mathrm{T}}$ is the vector of the unknown field variables, and $i, N_i, \boldsymbol{j}$ denote the external current, interpolation function and normalized current density defined so that $i\boldsymbol{j}$ corresponds to the current density. In addition, ν is the magnetic reluctivity which is the reciprocal of the permeability. In the homogenized region, we set $\langle\dot{\nu}\rangle = \langle\dot{\mu}\rangle^{-1}$ which represents the eddy current effect.

B. Time domain homogenized FEM

We convert (1) to time domain without introducing the auxiliary valuables relevant to the circuit equations. To do so, it is assumed that $\langle\dot{\nu}\rangle$ is expressed in the form of the continued fraction as

$$\langle\dot{\nu}\rangle = \frac{1}{\kappa_0} + \cfrac{1}{\cfrac{1}{s\kappa_1} + \cfrac{1}{\cfrac{1}{\kappa_2} + \cfrac{1}{\ddots}}} \triangleq \left[\frac{1}{\kappa_0}; \frac{1}{s\kappa_1}, \frac{1}{\kappa_2}, \frac{1}{s\kappa_3}, \cdots, \frac{1}{\kappa_{2q-2}}, \frac{1}{s\kappa_{2q-1}}\right] \tag{2}$$

which can be obtained by the unit cell approach proposed in [9] (see Appendix). We can obtain the time domain representation by applying the inverse Laplace transform $\mathcal{L}^{-1}[\cdot]$ to both side of (1). Then, we evaluate the term $\mathcal{L}^{-1}\left[\langle\dot{\nu}\rangle\dot{a}_j\right]$ by analogy with the circuit theory; we consider the correspondence $\langle\dot{\nu}\rangle/\mathrm{s} = \dot{Y}$, $s\dot{a}_j = \dot{V}$, $\langle\dot{\nu}\rangle\dot{a}_j = \dot{I}$ where $\dot{Y}, \dot{V}, \dot{I}$ are the admittance, current flowing $\dot{Y}$, and voltage across $\dot{Y}$, respectively. This analogy leads to the Cauer circuit shown in Fig. 1 because the continued fraction representation of $\dot{Y}$ corresponds to the admittance of the Cauer circuit. From Fig. 1, we readily obtain the circuit equations for the unknowns a_j as follows:

$$I(t) = \mathcal{L}^{-1}\left[\langle\dot{\nu}\rangle\dot{a}_j\right] = \frac{a_j(t)}{L_1} + I_1(t), \tag{3a}$$

$$\left(R + \frac{\mathrm{d}}{\mathrm{d}t}L\right)\boldsymbol{I}(t) = V(t)\boldsymbol{e}_1 = \frac{\mathrm{d}a_j(t)}{\mathrm{d}t}\boldsymbol{e}_1, \tag{3b}$$

$$R = \mathrm{diag}\left[R_1, R_2, \cdots, R_q\right], \tag{3c}$$

$$L = \begin{bmatrix} L_2 & -L_2 & & & & & \\ -L_2 & L_2 + L_3 & -L_3 & & & & \\ & -L_3 & L_3 + L_4 & -L_4 & & & \\ & & -L_4 & \ddots & \ddots & & \\ & & & \ddots & & & -L_q \\ & & & & & -L_q & L_q \end{bmatrix} \tag{3d}$$

where $R_i = 1/\kappa_{2i-1}$, $L_i = \kappa_{2i-2}$,and $\boldsymbol{I} = \left[I_1, I_2, \cdots, I_q\right]^{\mathrm{T}}$ are the resistances, inductances and loop currents in the Cauer circuit, and $\boldsymbol{e}_1$ denotes the first column of the unit matrix. By applying finite difference method to (3), we can express the current I^n at the n-th step in terms of the past variables as

$$I^n = \frac{a_j^n}{L_1} + I_1^n = \langle\nu\rangle a_j^n + \boldsymbol{e}_1^{\mathrm{T}}\left(R + \frac{1}{\Delta t}L\right)^{-1}\frac{-a_j^{n-1}\boldsymbol{e}_1 + L\boldsymbol{I}^{n-1}}{\Delta t}, \tag{4a}$$

$$\langle\nu\rangle = \left[\frac{1}{\kappa_0}; \frac{\Delta t}{\kappa_1}, \frac{1}{\kappa_2}, \frac{\Delta t}{\kappa_3}, \cdots, \frac{1}{\kappa_{2q-2}}, \frac{\Delta t}{\kappa_{2q-1}}\right], \tag{4b}$$

$$\boldsymbol{I}^n = \left(R + \frac{1}{\Delta t}L\right)^{-1}\left(\frac{a_j^n - a_j^{n-1}}{\Delta t}\boldsymbol{e}_1 + \frac{1}{\Delta t}L\boldsymbol{I}^{n-1}\right) \tag{4c}$$

where Δt denotes the time difference. Note that the first-order accurate backward difference is applied to (3) whereas the second-order accurate backward difference is used in the numerical result in Sec. III. By inserting (4a) into (1a), we obtain the time-domain equation which does not include the auxiliary valuables as follows:

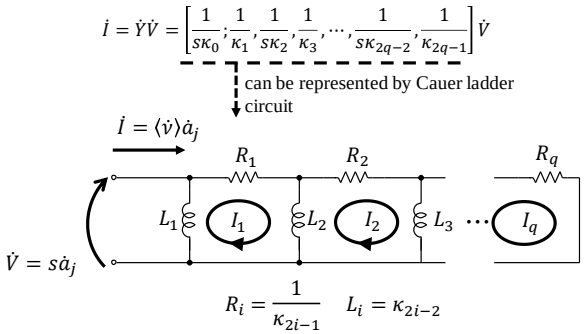

Fig.1. Continued fraction and corresponding Cauer equivalent circuit.

$$K(\langle\nu\rangle)\boldsymbol{x}^n = \boldsymbol{b}'i^n, \tag{5a}$$

$$\left(K\boldsymbol{x}^n\right)_i = \sum_j K_{ij}a_j^n = \sum_j \int_\Omega \mathrm{rot}\boldsymbol{N}_i \cdot \nu\mathrm{rot}\boldsymbol{N}_j d\Omega\, a_j^n, \tag{5b}$$

$$b_i' = \int_\Omega \boldsymbol{N}_i \cdot \boldsymbol{j}d\Omega + \sum_j \int_\Omega \mathrm{rot}\boldsymbol{N}_i \cdot c_j^{n-1}\mathrm{rot}\boldsymbol{N}_j d\Omega, \tag{5c}$$

$$c_j^{n-1} = \boldsymbol{e}_1^{\mathrm{T}}\left(R + \frac{1}{\Delta t}L\right)^{-1}\frac{a_j^{n-1}\boldsymbol{e}_1 - L\boldsymbol{I}_{\boldsymbol{j}}^{n-1}}{\Delta t} \tag{5d}$$

where $\nu = \langle\nu\rangle$ in the homogenized domain Ω_h. Note that we introduce the suffix j such as $\boldsymbol{I}_j^{n-1}$ because (3) holds for each unknown a_j. It is remarkable that the FE matrix in (5b) has the same form as that in (1b) while the former and latter are formulated in frequency and time domains, respectively. Updating the right-handed side vector by (5c) and (5d), the time domain analysis is performed stepwise.

C. Treatment of voltage input and power dissipation

The terminal voltage is computed from

$$v = \frac{\mathrm{d}}{\mathrm{d}t}\int_\Omega \boldsymbol{A} \cdot \boldsymbol{j}d\Omega + R_{DC}i = \frac{\mathrm{d}}{\mathrm{d}t}\boldsymbol{b}^{\mathrm{T}}\boldsymbol{x} + R_{DC}i. \tag{6}$$

where R_{DC} denotes the DC resistance of the winding. We can treat the voltage excitation by coupling (5a) with (6).

In frequency domain, the complex power is expressed as

$$\begin{aligned}\dot{P} &= \frac{s}{2}\int_{\Omega_h}\langle\nu\rangle^*|\boldsymbol{B}|^2 d\Omega + \frac{s}{2}\int_{\Omega\setminus\Omega_h}\nu|\boldsymbol{B}|^2 d\Omega + \frac{1}{2}R_{DC}I^2 \\ &= \frac{s}{2}\sum_{i,j\in\Omega_h}\int_{\Omega_h}\mathrm{rot}\boldsymbol{N}_i \cdot \mathrm{rot}\boldsymbol{N}_j d\Omega\,\langle\nu\rangle^*\dot{a}_i^*\dot{a}_j \\ &\qquad + \frac{s}{2}\int_{\Omega\setminus\Omega_h}\nu|\boldsymbol{B}|^2 d\Omega + \frac{1}{2}R_{DC}I^2.\end{aligned} \tag{7}$$

where $*$ represents the conjugate operator. Then, $s\langle\dot{\nu}\rangle^*\dot{a}_i^*\dot{a}_j$ in (7) are expanded as follows:

$$\begin{aligned}s\langle\dot{\nu}\rangle^*\dot{a}_i^*\dot{a}_j &= \dot{I}_i^*\dot{V}_j \\ &= s\frac{a_i^*a_j}{L_1} + \dot{\boldsymbol{I}}_{\boldsymbol{i}}^{\dagger}(R + sL)\dot{\boldsymbol{I}}_{\boldsymbol{j}} \\ &= \dot{\boldsymbol{I}}_{\boldsymbol{i}}^{\dagger}R\dot{\boldsymbol{I}}_{\boldsymbol{j}} + s\left(\frac{a_i^*a_j}{L_1} + \dot{\boldsymbol{I}}_{\boldsymbol{i}}^{\dagger}L\dot{\boldsymbol{I}}_{\boldsymbol{j}}\right)\end{aligned} \tag{8}$$

where † denotes the conjugate transpose operator $(\cdot)^{*\mathrm{T}}$. The first and second terms are real and purely imaginary because R, L are the symmetry matrices. Thus, the first term of (8) represents the Joule losses due to the eddy current. Consequently, we can compute the power dissipation in time domain from

$$W = \sum_{i,j\in\Omega_h} \int_{\Omega_h} \mathrm{rot}\boldsymbol{N}_i \cdot \mathrm{rot}\boldsymbol{N}_j d\Omega\, \boldsymbol{I}_i^{\mathrm{T}} R \boldsymbol{I}_j + R_{DC} I^2. \qquad (9)$$

III. Numerical Result

A. Validation on proposed method: linear case

For validation, we apply the proposed method to the FE analysis of the inductor which is composed of the multi-turn coil with 50 turns, wire radius 0.2 mm, and magnetic core, as shown in Fig. 2. The multi-turn is homogenized with the complex permeability in the form of continued fraction which represents the proximity effect in the coil. The number of the stage of the Cauer circuit q is set to 5, and the relative permeability of the magnetic core is here assume to be 2000. A sinusoidal current, unit amplitude, at 1 MHz is input to the inductor. It is assumed that $\Delta t = 0.01\ [\mu s], T = 3.0\ [\mu s]$. Although the skin effect can be considered by introducing the equivalent skin effect impedance Z_{skin} [2], it is neglected in the analysis for simplicity.

The power dissipation is plotted against time in Fig. 3. The relative error of the Joule losses per period is 1.2 % at largest. There are 19,485 nodes and 9,845 elements in the conventional FE model, whereas 8,073 and 4,151 in the homogenized model. The computational time, 2 min 11 sec, for the conventional FEM is reduced to 1 min 7 sec for the proposed method. Since the proposed method does not include the auxiliary variables in the FE equation, it is expected that its computational time is shorter than that of the method in [8] which solves the equation for the auxiliary variables. The reduction in computing time by the proposed method becomes more significant for 3D problems as will be shown below.

B. Validation on proposed method: nonlinear case

We apply the proposed method to the inductor considering the magnetic saturation. If eddy currents could flow in the core, we would introduce the nonlinear current-flux relation to the inductance in Fig.1, as presented in [8]. The inductor is excited by the sinusoidal voltages, 200 and 400 V, at 100 kHz. It is assumed that $\Delta t = 0.1\ [\mu s], T = 30\ [\mu s]$. The power dissipation is plotted versus time in Fig. 4. We can see that the results obtained by the proposed method is in good agreement with those obtained by the conventional FEM. The waveform for 400 V is deeply distorted by the magnetic saturation.

C. 3D inductor model

The proposed method is applied to the 3D inductor model shown in Fig. 5. The turn number and wire radius are the same as those in the 2D model and magnetic saturation is considered.

Table I
Values in continued fraction which is computed by unit cell approach

i	κ_{2i-2}	κ_{2i-1}
1	1.000×10^{0}	3.635×10^{-7}
2	8.246×10^{-1}	3.119×10^{-8}
3	2.244×10^{0}	5.569×10^{-9}
4	5.251×10^{0}	1.076×10^{-8}
5	1.040×10^{2}	1.762×10^{-9}

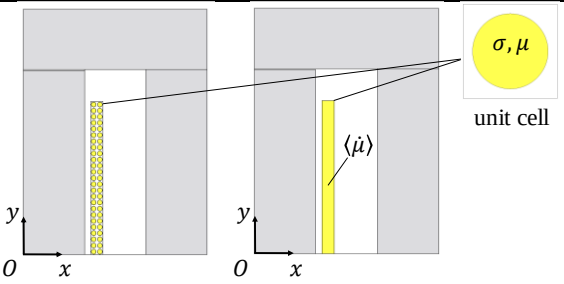

Fig.2. Conventional (left) and homogenized inductor model (2D).

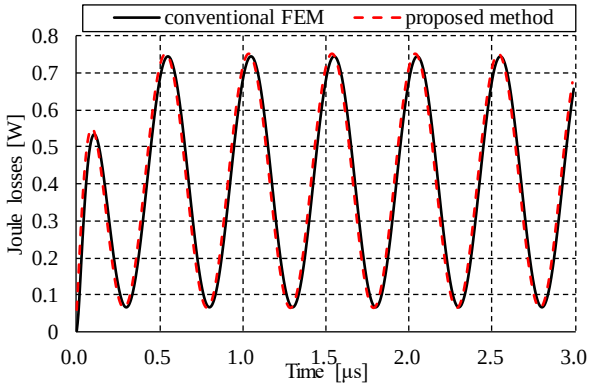

Fig. 3. Power dissipation versus time obtained with conventional and homogenized FEM. The magnetic core with constant permeability is considered with sinusoidal current input at 1 MHz.

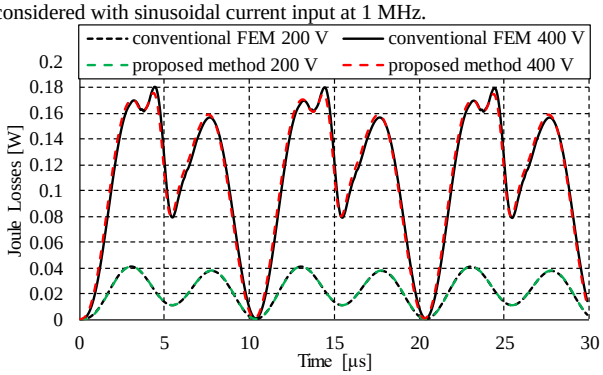

Fig. 4. Power dissipation versus time obtained with conventional and homogenized FEM. The saturable magnetic core is considered with sinusoidal voltage input at 100 kHz.

It needs large computing cost to analyze this model using the conventional FEM; there would be more than 4,000,000 elements when skin depth at 100 kHz is considered. On the other hand, the homogenized model requires only 173,866 elements and 210,676 edges. A pulsatile, 1 V, at 100 kHz, duty factor 0.5, shown in Fig.6, is input to the inductor. The load resistance is assumed 2 Ohm. It is assumed that $\Delta t = 0.1\ [\mu s]$, $T = 30\ [\mu s]$.

The power dissipation and current of the inductor are plotted against time in Fig. 6 and Fig. 7. For comparison, the Joule losses of the inductor due to DC resistance is also plotted in the figure. During periods $T \in [0, 5], [10, 15], [20, 25]$, the current increases linearly and the DC loss has the quadratic increase

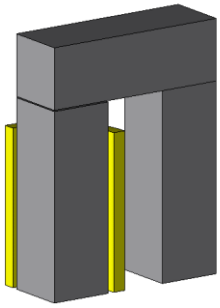

Fig. 5. 3D inductor model. One-eight domain is considered.

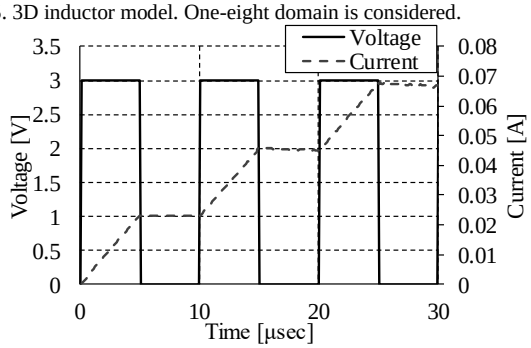

Fig. 6. Waveforms of input voltage and output current.

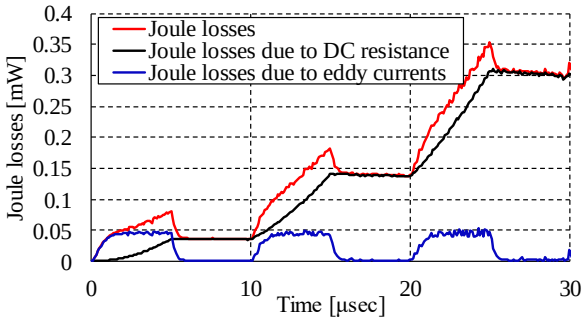

Fig. 7. Power dissipation and current versus time obtained with homogenized FEM. The inductor with a saturable magnetic core is excited by pulse voltage at 100 kHz, duty factor 0.5, amplitude 3 V.

whereas the Joule losses obtained by the proposed method has fairly complicated waveform due to the proximity effect. During period $\mathrm{T} \in [5,10],[15,20],[25,30]$, the current becomes constant, therefore, the Joule losses obtained by the proposed method has the nearly same value as the DC loss because there is no time variation in the electromagnetic field.

IV. Conclusion

In this paper, we proposed a new method for the time domain homogenization analysis based on the continued fraction representation of the complex permeability. The novelty of this method is in the elimination of the auxiliary variables for the circuit equation. The Joule losses obtained by the proposed method has enough accuracy compared with those obtained by the conventional FEM. The proposed method is effective especially for 3D models. In future, we plan to extend the proposed method to treat iron sheets.

Appendix

The complex permeability in the form of continued fraction can be obtained by using the method proposed by the authors [9]. The method utilizes the energy representation of the complex permeability which is reduced to the continued fraction using the Cauer via Lanczos (CVL) [10], one of model order reduction techniques. The algorithm of CVL is also described in [9].

The energy representation of the complex permeability is given as

$$\langle \dot{\mu} \rangle = \frac{\int_\Omega |\boldsymbol{B}_0|^2 \mathrm{d}\Omega}{\int_\Omega \frac{|\boldsymbol{B}|^2}{\mu}\mathrm{d}\Omega - \frac{1}{\mathrm{j}\omega}\int_\Omega \sigma |\boldsymbol{E}|^2 \mathrm{d}\Omega} = \frac{\int_\Omega |\boldsymbol{B}_0|^2 \mathrm{d}\Omega}{\int_{\partial\Omega} \boldsymbol{E}^* \times \boldsymbol{H} \cdot \boldsymbol{n} \mathrm{d}S} \tag{A1}$$

which is derived from the requirement that the energies in the original and homogenized unit cells are equal. The FE discretization of (A1) results in

$$\langle \dot{\mu} \rangle = \frac{V}{\boldsymbol{c}^{\mathrm{T}}(K + sN)^{-1}\boldsymbol{b}} \tag{A2}$$

where $\mathrm{V} = \int_\Omega d\Omega$ denotes the volume of the unit cell. The transfer function in (A2) is approximated by the continued fraction using CVL. Therefore, we can obtain the continued fraction representation (2).

Acknowledgment

This work was supported in part by JSPS KAKENHI Grant Number JP1920541 and 18H01664.

References

[1] J. Gyselinck and P. Dular, "Frequency-domain homogenization of bundles of wires in 2-D magnetodynamic FE calculations," *IEEE Trans. Magn.*, vol. 41, no. 5, pp. 1416–1419, May 2005.

[2] H. Igarashi, "Semi-Analytical Approach for Finite-Element Analysis of Multi-Turn Coil Considering Skin and Proximity Effects," *IEEE Trans. Magn.*, vol. 53, no. 1, pp. 1–7, Jan. 2017.

[3] A. D. Podoltsev, I. N. Kucheryavaya, and B. B. Lebedev, "Analysis of effective resistance and eddy-current losses in multiturn winding of high-frequency magnetic components," *IEEE Trans. Magn.*, vol. 39, no. 2, pp. 539–548, 2003.

[4] A. T. Phung, G. Meunier, O. Chadebec, X. Margueron, and J. P. Keradec, "High-frequency proximity losses determination for rectangular cross-section conductors," *IEEE Trans. Magn.*, vol. 43, no. 4, pp. 1213–1216, Apr. 2007.

[5] G. Meunier, V. Charmoille, C. Guérin, P. Labie, and Y. Maréchal, "Homogenization for periodical electromagnetic structure: Which formulation?," *IEEE Trans. Magn.*, vol. 46, no. 8, pp. 3409–3412, Aug. 2010.

[6] J. Gyselinck and P. Dular, "A time-domain homogenization technique for laminated iron cores in 3-D finite-element models," *IEEE Trans. Magn.*, vol. 40, no. 2 II, pp. 856–859, Mar. 2004.

[7] J. Gyselinck, R. V. Sabariego, and P. Dular, "Time-domain homogenization of windings in 2-D finite element models," *IEEE Trans. Magn.*, vol. 43, no. 4, pp. 1297–1300, Apr. 2007.

[8] Y. Sato and H. Igarashi, "Time-Domain Analysis of Soft Magnetic Composite Using Equivalent Circuit Obtained via Homogenization," *IEEE Trans. Magn.*, vol. 53, no. 6, pp. 1–4, 2017.

[9] S. Hiruma and H. Igarashi, "Homogenization Method Based on Cauer Circuit via Unit Cell Approach," *IEEE Trans. Magn.*, DOI: 10.1109/TMAG.2019.2946402 Manuscript Number: MAGCON-19-08-0351.

[10] S. Hiruma and H. Igarashi, "A study on orthogonal polynomials and Stieltjes continued fraction," *Papers Joint Tech. Meeting Static App. Rotating Mach. IEE Japan*, SA-18-013, pp.1-8, 2018, (in Japanese).